Evaluating leakage from radial lip seals affected by bearing area of shaft topography

Evaluating leakage from radial lip seals affected by bearing area of shaft topography

Kozuch E, M.Sc.[1], Nomikos P, MOE.[1,2], Rahmani R, PhD.[1], Morris N, PhD.[1], Rahnejat H, PhD.[1]

[1] Wolfson School of Mechanical, Manufacturing and Electrical Engineering, Loughborough University, Leicestershire, UK

[2] Neapco Europe GmbH, Germany

Summary

This paper investigates the influence of shaft surface topography upon seal leakage, when using different surface finishing and manufacturing techniques. A hydrodynamic model is used to determine the generated pressure distribution within the seal-shaft contact. Pertinent statistical parameters are selected to distinguish between the various shaft surface topographies, which can contribute to an effectively sealed conjunction. Results obtained from the hydrodynamic model shows the creation of multiple cavitated regions caused by the deep valleys. This leads to thinner film thickness on the surface plateau and therefore lower predicted leakage rates. The distribution of peaks and valleys is shown to be a factor in differentiating contact performance.

1 Introduction

Radial lip seals are widely used in the automotive industry as an effective sealing solution for the gearbox, transaxle and differentials. The simplicity of their design and the low manufacturing cost makes them preferable to other seal types. Ideally, when installed the seal should prevent leakage of lubricant during the relative motion of the shaft and the seal, owing to the angular motion of the shaft and its radial vibrations.

A significant amount of research has been devoted to the improvement of radial lip seals. For example, the understanding of reverse pumping, resulting from the shear of the seal surface asperities is very important. Commonly the shaft counterface is rather smoother in comparison with the seal surface; therefore, its topography is usually ignored in the developed models /1-3/. Nevertheless, deteriorating performance with increasing shaft roughness or extensive polishing has been mentioned and studied /4-6/, resulting in establishing an optimum range of surface roughness parameters, specifically square root mean heights, R_q and maximum height, R_z. These have been incorporated into all the main standards /7, 8/ used in industry.

Although the vast majority of shafts meet the specified topography and no appreciable lead is created on the surface, significant variations in performance have been observed. These lead to the conclusion that not only average height and range of heights, but also their distribution should be considered as previously suggested by Shen /9/. General studies of non-Gaussian surfaces have shown that deviations in skewness, R_{sk} and kurtosis, R_{ku} can induce cavitation and alter the regime of lubrication through thin fluid films affecting friction and load carrying capacity /10,11/. The skewness indicates existence of deep valleys and high peaks and kurtosis is a measure of concentration of heights distribution. A similar trend can be observed from the Abbott-Firestone material ratio curve as noted by Almqvist et al /12/. Widely used in industry, the ISO 13565 /13/ specifies core parameters such as the Kernel roughness depth, R_k, the reduced peak height, R_{pk} and reduced valley height, R_{vk} which give clear indications of the nature of surface asperity distribution. Although distribution parameters described in ISO 4287/14/ are obtained using different approaches to the core parameters, a similar trend can be seen when comparing skewness and ratio of the upper area, $A1$ to the lower area, $A2$ obtained from material ratio curves. Skewness for Gaussian surfaces would have a value of zero and a negative value corresponds to the height distribution skewed towards deeper valleys and lower peaks. This indicates that the ratio of $A1$ to $A2$ would be less than unity. Positive skewness would be represented by a ratio of $A1$ to $A2$ exceeding unity.

In this paper the investigated shaft surfaces are described using the core topographical parameters. A hydrodynamic model is developed to ascertain whether the aforementioned area ratios can be directly related to a change in the regime of lubrication with the thin fluid films.

2 Surface measurements

Three shafts with the same average roughness specification were manufactured using different surface-finish processes. All the shafts' surfaces were measured in order to comprehensively compare their topographies. An optical interferometer with x100 magnification lens is used, providing resolution of 20nm in the vertical direction (normal to the surfaces) and 1μm in the lateral directions (i.e. along the surfaces). All the measured sample surface regions had an area of 110μm x 145μm. The objective was chosen to match the measured areas with the predicted axial contact width of the real shaft seal footprint conjunction, thus allowing identification of contact specific roughness characteristics. The measured area serves as a low frequency filter of the surface topography. Figure 1 shows a set of the parameters with averaged values and their standard deviation taken from 15 measurements where, S_q is the surface root mean square height, S_k is the surface core roughness depth, S_{pk} is surface reduced peak height and S_{vk} is the surface reduced valley height.

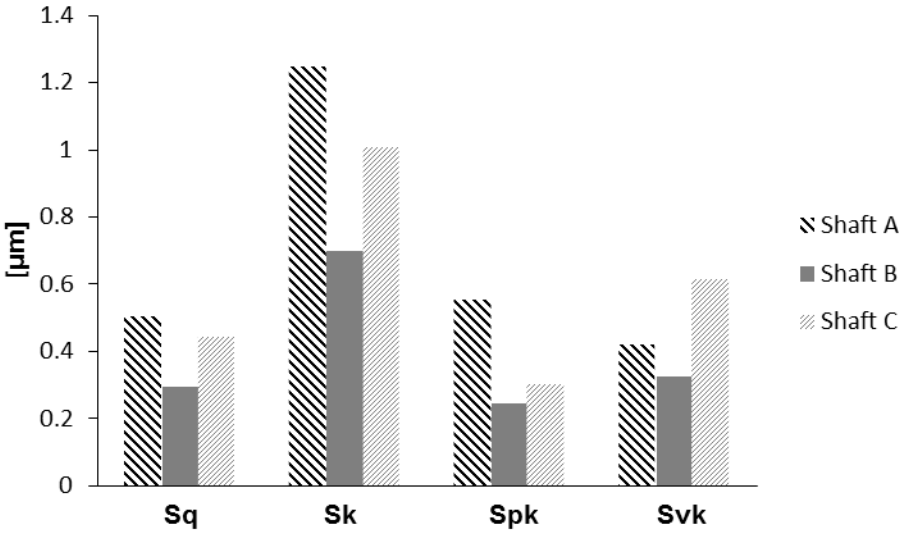

Figure 1: Surface roughness parameters: S_q, S_k, S_{pk}, and S_{vk}

In practice, it has been observed that Shaft A exhibits the lowest performance of the three shaft surface types, with a higher propensity for leakage. A better performance is obtained from Shaft B, whilst Shaft C is found to give the best performance. From the results in Figure 1, it is not possible to find an association between the investigated topographical parameters and the in-field reported performance of the shaft types. However, if one takes the ratio of the upper volume $Sa1$ and lower volume $Sa2$ found from the Abbott-Firestone curves shown in Figure 2, it is possible to find the ratio of the high peaks area (above core) to the bearing area (below the core/plateau). Figure 3 shows the ratio of these areas, demonstrating the tendency of better performance of surfaces with larger bearing valley volumes, or reduced peak heights. Figure 2 gives an example of the comparison of two measured samples taken from Shaft A (Figure 2a) and Shaft C (Figure 2b) where clear area ratio differences are observed.

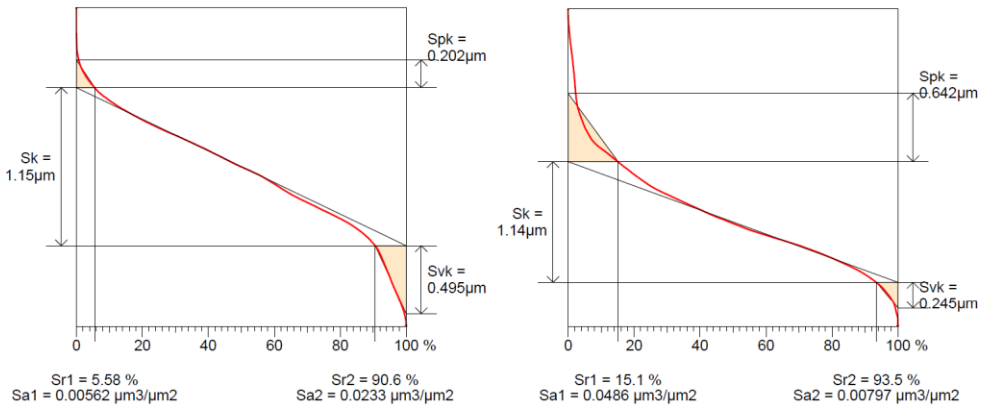

Figure 2: Comparison of surface material ratio curves: (a) Shaft A sample and (b) Shaft C sample

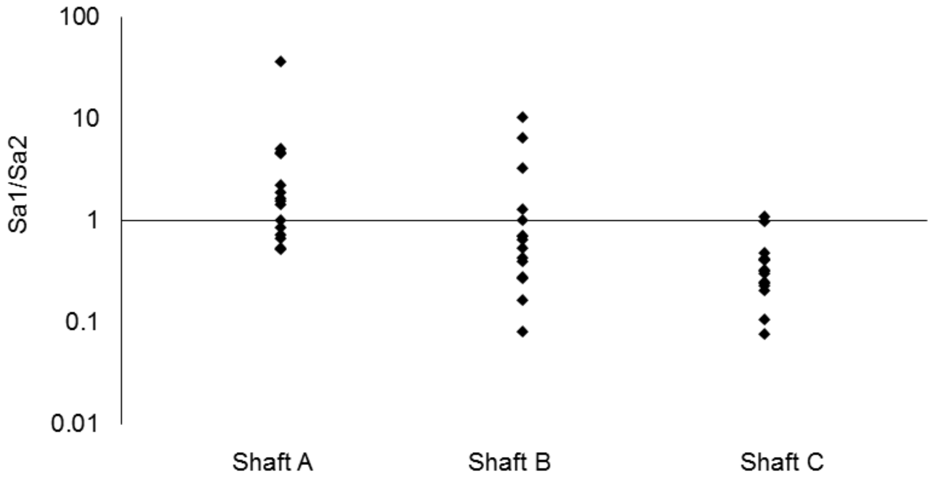

Figure 3: Ratio of volume above core (high peaks) to volume below core (deep valleys) obtained from material ratio curve

Leakage occurs in the axial direction. Therefore, 2D profiles were extracted from the middle of the measured topographical surface areas and the roughness parameters compared. Again, the same trends were observed as in the case of the 3D surface samples. Therefore, the investigation of hydrodynamic lubrication and leakage using numerical model can be simplified through 1D analysis along the axial direction only with a good degree of accuracy.

3 Numerical model

A 1D hydrodynamic model is developed, based on Reynold's equation commonly used for thin fluid films /15-17/. 10 shaft profiles were extracted from the measured surfaces and chosen, based on similar R_a and R_z parameters, but differentiated by their peaks to valleys area $A1/A2$ ratio. Half of the profiles had mentioned area ratio greater than unity and the other half lower than unity. For each profile the hydrodynamic load, cavitated regions and predicted leakage were investigated. Figure 4 is a schematic representation of the model.

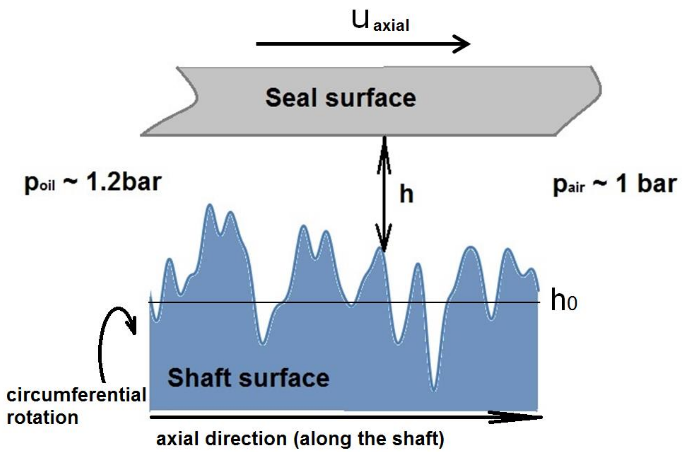

Figure 4: Schematic representation of considered rough shaft – smooth seal conjunction

The one dimensional assumption means that the relative rotational speed is not considered, although the axial movement is introduced to determine the differences in the generated hydrodynamic pressure fluctuations and imitate real working conditions where axial vibrations are common place. The minimum fluid film thickness between the surfaces was not set allowing the separation of the counter surfaces to adjust to the externally applied load. This mimics the real in situ conditions, where the mounting load and the hydrodynamic reaction equilibrate at a specific fluid film thickness (gap). For the purpose of this work, the load applied was small enough to produce a coherent hydrodynamic lubricant film in the cases investigated. However, in practice there is a likelihood of direct asperity interactions at certain operating conditions.

Finally, due to focus on shaft topography and its influence on the generated hydrodynamic pressure distribution, the seal was treated as perfectly flat and smooth. Therefore the reverse pumping effect is ignored in the current study. To isolate the effect of shaft topography upon lubrication, this assumption is regarded as a reasonable initial step.

The fluid film pressure distribution is obtained through discretisation of the governing equation using central finite differences and over-relaxation point successive Gauss-Seidel iterative method. The pressure at the boundary was set to atmospheric pressure on the external side and slightly above atmospheric on oil side of the seal. The cavitation pressure was set to the atmospheric pressure.

Figure 5 presents a pressure distribution with clearly visible cavitation regions which are encouraged due to the divergent gaps in the contacting profile with deep valleys. Figure 6 corresponds to a profile with higher asperity peaks, where pressure builds up instead of fluctuating as in Figure 5. This accumulation pressure rises akin to the partial surface texturing effect, leading to a higher mean gap between the seal and the shaft. Consequently, higher mean gaps results in higher flow rates in Figure 7, causing a greater tendency for seal leakage as seen in Figure 8.

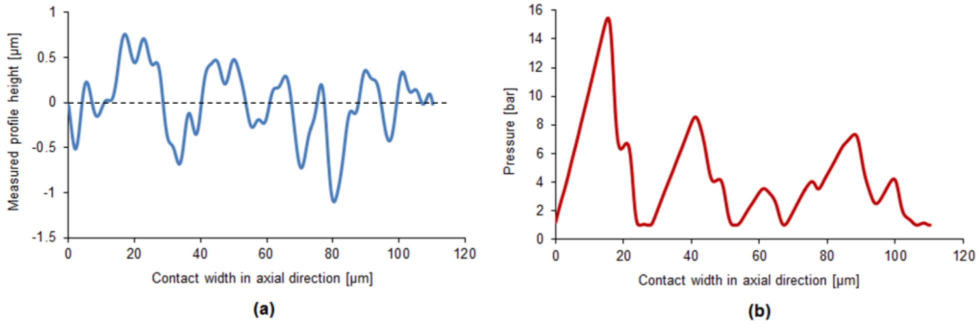

Figure 5: (a) Profile with higher S_{vk} and (b) the corresponding pressure distribution

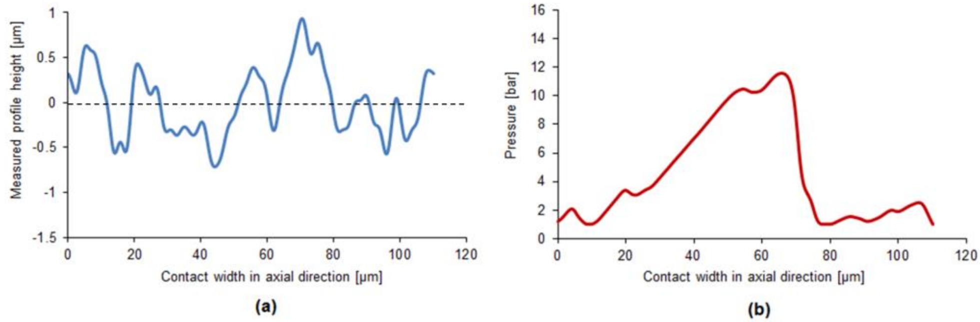

Figure 6: (a) Profile with higher S_{pk} and (b) the corresponding pressure distribution

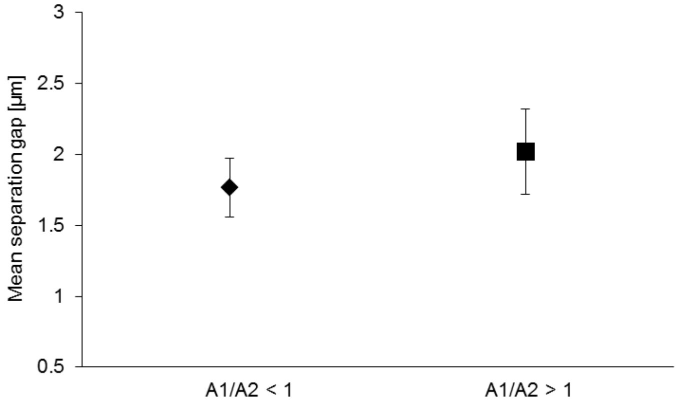

Figure 7: Mean separation gap between the seal and shaft surfaces

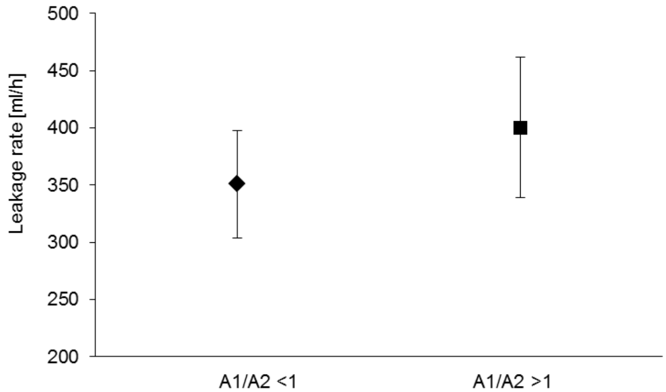

Figure 8: Average flow rate in the axial direction

4 Summary and Conclusions

As observed from the numerical predictions, topographic profiles with deeper valleys cause high fluctuations in generated pressures with frequent pressure drops which can result in cavitation. The profiles containing higher asperity peaks tend to generate higher fluid film pressures. Deep valleys create reservoirs of lubricant and thinner mean gaps between the seal and the shaft. Shaft profiles consisting of high peaks tend to push the seal away, leaving much wider surface separations, allowing the lubricant to flow through the contact with great ease. Therefore, based on a pure hydrodynamic analysis, shafts of higher bearing area $A2$ would perform better than those with higher peaks area, $A1$. To perform full analysis, one would include reverse pumping effect as a factor to distinguish between acceptable and failing levels of $A1/A2$ ratio, as well as the effect of shaft asperities on the load carrying capacity and wear of the seal surface during the running-in period.

5 Acknowledgements

The authors are grateful to the Engineering and Physical Science Research Council (EPSRC) for the financial support extended to this research through the Doctoral Training Program (DTP) scheme. The authors also acknowledge the contribution made by the indusial partner of the project.

6 Nomenclature

Variable	***Description***	***Unit***
$A1$	Material ratio curve upper area	[μm^2/μm]
$A2$	Material ratio curve lower area (bearing area)	[μm^2/μm]
R_a	Arithmetic mean of asperity heights	[μm]
R_k, S_k	Kernel roughness depth of the profile	[μm]
R_{ku}	Kurtosis	[-]
R_{pk}, S_{pk}	Reduced peak height	[μm]
R_q, S_q	Square root mean of asperity heights	[μm]
R_{sk}	Skewness	[-]
R_{vk}, S_{vk}	Reduced valley height	[μm]
R_z	Maximum height	[μm]
$Sa1$	Material ratio curve upper volume	[μm^3/μm^2]
$Sa2$	Materia ratio curve lower volume	[μm^3/μm^2]

7 References

/1/ Harp, S.R. and Salant, R.F., *Inter-asperity cavitation and global cavitation in seals: An average flow analysis*, Tribology International, Vol. 35/2, pp. 113-121, 2002.

/2/ Salant, R.F. and Rocke, A.H., *Hydrodynamic analysis of the flow in a rotary lip seal using flow factors*, Journal of Tribology, Vol. 126/1, pp.156-161, 2004.

/3/ Guo, F., Jia, X., Suo, S., Salant, R.F. and Wang, Y., *A mixed lubrication model of a rotary lip seal using flow factors*, Tribology International, Vol. 57/1, pp.195-201, 2013.

/4/ Jagger, ET., *Rotary shaft seals: the sealing mechanism of synthetic rubber seals running at atmospheric pressure*, Proceedings of IMechE, Vol. 171/,1, pp. 597-616, 1957.

/5/ Salant, R.F. and Shen, D., *Hydrodynamic effects of shaft surface finish on lip seal operation*, Tribology Transactions, Vol. 45/3, pp. 404-410, 2002.

/6/ Schulz, M., Baumann, M., Bauer, F., *Influence of belt ground and superfinished shaft counterfaces on the tribological and functional behavior of elastomeric lip seals,* Proceedings of 24th International Conference on Fluid Sealing, BHR Group, Manchester, UK, 2018.

/7/ BS ISO 6194-1:2007, *Rotary shaft lip-type seals incorporating elastomeric sealing elements - Part 1: Nominal dimensions and tolerances*, 2007, https://www.iso.org/standard/34678.html

/8/ RMA OS 1-1:2004, *Oil seal technical bulletin – shaft requirements for rotary lip seals*, 2004, https://infostore.saiglobal.com/en-gb/standards/rma-os-1-1-2004-570592/.

/9/ Shen, D., *Deterministic modeling of a rotary lip seals with microasperities on the shaft* surface, PhD thesis, Georgia Institute of Technology, USA, 2005.

/10/ Sedlacek, M., Podgornik, B., Vizintin, J., *Correlation between standard roughness parameters skewness and kurtosis and tribological behaviour of contact surfaces*, Tribology International, Vol. 48/4, pp.102-112, 2012.

/11/ Andharia, P.I., Gupta, J.L., Deheri, G.M., *Effect of surface roughness on hydrodynamic lubrication of slider bearing*, Tribology Transactions, Vol. 44/2, pp.291-297, 2001.

/12/ Almqvist, A., Sahlin, F., Larsson, R., Glavatskih, S., *On the dry elasto-plastic contact of nominally flat surfaces,* Tribology International, Vol. 40, pp.574-579, 2007

/13/ ISO 13565-2:1996, *Geometrical Product Specifications (GPS) - Surface texture: Profile method; Surfaces having stratified functional properties - Part 2: Height characterization using the linear material ratio curve*, 1996, https://www.iso.org/standard/22280.html

/14/ ISO 4287:1997, *Geometrical Product Specifications (GPS) - Surface texture: Profile method - Terms, definitions and surface texture parameters*, 1997, https://www.iso.org/standard/10132.html

/15/ Gohar, R. and Rahnejat, H., *Fundamentals of tribology*, Imperial College Press, London, UK, 2012.

/16/ Rahmani, R. and Rahnejat, H., *Enhanced performance of optimised partially textured load bearing surfaces*, Tribology International, Vol. 117/1, pp.272-282, 2018.

/17/ Morris, N., Shahmohamadi, H., Rahmani, R., Rahnejat, H. and Garner, C.P., *Combined experimental and multiphase computational fluid dynamics analysis of surface textured journal bearings in mixed regime of lubrication,* Lubrication Science, Vol. 30/6, pp.161-173, 2018.